

Neutrino mass hierarchy extraction using atmospheric neutrinos in ice

Olga Mena^{1,2}, Irina Mocioiu³ and Soebur Razzaque⁴

¹ *INFN Sez. di Roma, Dipartimento di Fisica, Università di Roma “La Sapienza”, P.le A. Moro, 5, I-00185 Roma, Italy*

² *Institute of Space Sciences(IEEC-CSIC), Fac. Ciencies, Campus UAB, Bellaterra, Spain*

³ *Department of Physics, Pennsylvania State University, University Park, PA 16802, USA and*

⁴ *Space Science Division, Code 7653, U.S. Naval Research Laboratory, Washington DC 20375, USA*

(Dated: May 28, 2019)

We show that the measurements of 10 GeV atmospheric neutrinos by a proposed array of densely-packed phototubes buried deep inside the IceCube detector at the South Pole can be used to determine the neutrino mass hierarchy for an extended region of the parameter space.

PACS numbers: 14.60.Pq

I. INTRODUCTION

Neutrino physics has undergone a true revolution over the last decade, with a large number of experiments of different types providing evidence for neutrino oscillations and thus for physics beyond the Standard Model. This has led to new insights into the possibilities for new physics, but while some old questions have been answered, many new questions have emerged [1].

An important question that still needs to be resolved is the determination of the neutrino mass hierarchy. A very large effort has been dedicated to planning new experiments for measuring all neutrino oscillation parameters [2]. The mass hierarchy can be determined using matter effects on oscillations inside the Earth. This however requires a long baseline, a very large detector and an intense beam. In addition, parameter degeneracies have to be resolved using a combination of experiments.

Cosmic ray interactions in the atmosphere give a natural beam of neutrinos. These atmospheric neutrinos in the GeV range have been used by the Super-Kamiokande detector to provide evidence for neutrino oscillations. The large size of neutrino telescopes such as AMANDA, IceCube and KM3NeT makes possible the detection of a large number of atmospheric neutrino events with a higher energy threshold, ~ 100 GeV, even though the neutrino flux decreases rapidly with energy ($\sim E_\nu^{-3}$). Built to detect neutrinos from astrophysical sources, dark matter annihilation, etc. [3], these ice/water Cherenkov detectors typically have high detection threshold energy to avoid the large background from atmospheric neutrinos. Since neutrino oscillation effects are quite small at high energies, high energy atmospheric neutrinos provide little information about important issues such as neutrino mass hierarchy, mixing angles, etc.

Recently, a low energy extension of the IceCube detector has been proposed [4]. Its goal is to significantly improve the atmospheric muon rejection and to extend the IceCube neutrino detection capabilities in the low energy domain, possibly to muon energies as low as 5 GeV, depending on the density of the photo tubes. The proposed instrumented volume is 5,000-10,000 kton by conservative estimates. Such a low threshold array buried deep inside IceCube will open up a new energy window

on the universe. It will search for neutrinos from sources in the Southern hemisphere, in particular from the galactic center region, as well as for neutrinos from WIMP annihilation, as originally motivated. Here we provide an additional and independent motivation for building such an array, namely to explore neutrino oscillation physics.

In this article we show that the deep core extension of IceCube provides a great opportunity for detailed oscillations studies of atmospheric neutrinos and makes possible the determination of the neutrino mass hierarchy. This is extremely important given that long baseline experiments with comparable sensitivity might take a very long time to build and collect data, while the IceCube deep core will be built in the near future and will accumulate high statistics relatively fast. Our study indicates that for a total mass of the instrumented volume times exposure of 100 Mt yr (roughly equivalent to 10 years of running such a 10,000 kton detector), neutrino mass hierarchy can be determined at least with 90% confidence level assuming the current best-fit values of the oscillation parameters, and for a range of allowed values of θ_{13} .

We start in section II with a brief review of what we know about neutrino oscillation parameters and what we expect to learn in the near future. We also discuss matter effects inside the Earth, which play an important role in the analysis. In section III we describe our main analysis and in section IV we discuss the backgrounds and systematic uncertainties that affect this analysis. We present the main results in section V and discuss them in section VI.

II. NEUTRINO OSCILLATIONS

Neutrino data from solar, atmospheric, reactor and accelerator experiments is well understood in terms of three-flavour neutrino oscillations. Two Δm^2 values and two (large) mixing angles are well determined, while the third mixing angle is limited to be very small. The CP-violating phase (δ) is completely unconstrained. In addition, the sign of Δm_{31}^2 is also unknown and will be the focus of our study. The two possibilities, $\Delta m_{31}^2 > 0$ or $\Delta m_{31}^2 < 0$ correspond to two types of neutrino mass ordering, normal hierarchy and inverted hierarchy.

The best fit oscillation parameter values obtained from present data are [2, 5]:

$$|\Delta m_{31}^2| = 2.5 \times 10^{-3} \text{eV}^2 \quad (1)$$

$$\Delta m_{21}^2 = 8 \times 10^{-5} \text{eV}^2 \quad (2)$$

$$\sin^2 2\theta_{23} = 1 \quad (3)$$

$$\tan^2 2\theta_{12} = 0.45 \quad (4)$$

with 99% CL allowed regions given by:

$$|\Delta m_{31}^2| \in (2.1 - 3.1) \times 10^{-3} \text{eV}^2 \quad (5)$$

$$\Delta m_{21}^2 \in (7.2 - 8.9) \times 10^{-5} \text{eV}^2 \quad (6)$$

$$\theta_{23} \in (36^\circ - 54^\circ) \quad (7)$$

$$\theta_{12} \in (30^\circ - 38^\circ) \quad (8)$$

and $\sin^2 2\theta_{13} \leq 0.15$ for $\Delta m_{31}^2 = 2.5 \times 10^{-3} \text{eV}^2$. Notice that an extra unknown in the neutrino oscillation scenario is the octant in which θ_{23} lies, if $\sin^2 2\theta_{23} \neq 1$. This has been dubbed in the literature as the θ_{23} octant ambiguity.

In the near future, long baseline experiments like MINOS and OPERA will improve the current precision on Δm_{31}^2 and possibly discover a non-zero value of θ_{13} , if this is close to the present upper limit. In a few years, reactor experiments like DoubleChooz and DayaBay will provide improved sensitivity to θ_{13} . This information can be used as input in our analysis, reducing some of the parameter uncertainties.

In the past, atmospheric neutrinos in the Super-Kamiokande detector have provided evidence for neutrino oscillations and the first measurements of $|\Delta m_{31}^2|$ and $\sin^2 2\theta_{23}$. It is also known that, covering a large range of energies and pathlengths and using matter effects inside the Earth, they can be in principle sensitive to sub-dominant neutrino oscillation effects like θ_{13} and the mass hierarchy [6, 7, 8, 9, 10, 11, 12, 13].

Matter effects [19, 20] in long baseline and atmospheric neutrino oscillation experiments depend on the size of the mixing angle θ_{13} which governs the transitions $\nu_e \leftrightarrow \nu_{\mu, \tau}$ driven by the atmospheric mass squared difference $\Delta_{31} = \Delta m_{31}^2/2E$. The effective θ_{13} mixing angle in matter in a two-flavour framework is given by:

$$\sin^2 2\theta_{13}^m = \frac{\sin^2 2\theta_{13}}{\sin^2 2\theta_{13} + \left(\cos 2\theta_{13} \mp \frac{\sqrt{2}G_F N_e}{\Delta_{31}} \right)^2}, \quad (9)$$

where the minus (plus) sign refers to neutrinos (antineutrinos), N_e is the electron number density in the medium, $\sqrt{2}G_F N_e$ (eV) = $7.6 \times 10^{-14} Y_e \rho$ (g/cm³) and Y_e , ρ the electron fraction and the density of the medium, the Earth interior in our case. The electron fraction Y_e is 0.466 (0.494) in the core (mantle) and we follow the PREM [21] model for the Earth's density profile. Equation (9) implies that, in the presence of matter effects, the neutrino (antineutrino) oscillation probability gets enhanced if the hierarchy is normal (inverted). Making use of the different matter effects for neutrinos and antineutrinos seems therefore the ideal way to distinguish

among the two possibilities: normal versus inverted mass hierarchy. Matter effects are expected to be important when the resonance condition:

$$\Delta m_{31}^2 \cos(2\theta_{13}) = 2\sqrt{2}G_F N_e E, \quad (10)$$

is satisfied. The precise location of the resonance will depend on both the neutrino path and the neutrino energy. For $\Delta m_{31}^2 \sim 2.5 \times 10^{-3} \text{eV}^2$ and distances of several thousand kilometers the resonance effect is expected to take place for neutrino energies $\mathcal{O}(10)$ GeV. The pathlength traveled by atmospheric neutrinos is:

$$L(c_\nu) = R_\oplus (\sqrt{(1 + l/R_\oplus)^2 - s_\nu^2} - c_\nu), \quad (11)$$

where $R_\oplus = 6371$ km is the radius of the Earth and $l \sim 15$ km is the typical height at which neutrinos get produced in the atmosphere. The cosine and sine of the nadir angle of the incident neutrino are denoted by c_ν and s_ν , respectively. Since *upward going* ($c_\nu \rightarrow -1$) atmospheric neutrinos traverse the dense core of the Earth, they provide an excellent tool to tackle the neutrino mass ordering.

Indeed the idea of exploiting matter effects in atmospheric neutrino oscillations to distinguish the type of hierarchy has been extensively explored in the literature [6, 7, 8, 9, 10]. In general, the former studies exploit muon calorimeter detectors, such as MONOLITH [16], MINOS [17] or INO [18] in which the muon charge can be determined. The measurement of the number of positive and negative muons in the 1 – 10 GeV energy region allows then for a direct extraction of the neutrino mass hierarchy, simply by looking in which channel (neutrino or antineutrino) the signal, via matter effects, is enhanced. However, it has been pointed out, and carefully explored, that the detection of atmospheric neutrinos which have crossed the Earth by future planned megaton water Cherenkov detectors could also determine the neutrino mass hierarchy, provided the mixing parameter $\sin^2 2\theta_{13}$ is not very small [11, 12, 13], even when these detectors do not allow for a charge discrimination of the leptons. The detection of *low energy* neutrinos in a higher density photo-multiplier array within the IceCube instrumented detector volume opens up the possibility of not only exploring the atmospheric oscillation pattern [15], but also exploring how well the neutrino mass hierarchy could be measured in the *largest* water/ice Cherenkov detector available in the near future. In the next section we present the details of the analysis proposed here. For our numerical analysis, unless otherwise stated, we will use the best fit values quoted earlier in this section for the oscillation parameters.

III. ANALYSIS

The IceCube detector has the ability to measure separately the muon tracks and electron/tau generated cascades, thus providing good flavour identification in some

energy ranges. This would be extremely useful for an oscillation analysis, especially when searching for subdominant effects. In particular, the atmospheric neutrino sensitivity to the mass hierarchy comes from the matter effects on $\nu_\mu \rightarrow \nu_e$ ($\bar{\nu}_e \rightarrow \bar{\nu}_\mu$) oscillations and previous studies dealing with water Cherenkov detectors have used the electron signal to extract this information. In the low energy range relevant for neutrino oscillations however,

it is extremely hard in IceCube (and even in the deep core array) to obtain information about neutrino direction and energy for electron cascades.

We thus focus here on the μ -like *contained* events produced by the interactions of atmospheric upward going neutrinos in deep ice. Formally, the expected number of muon neutrino-induced contained events in the i - and j -th energy and cosine of the nadir angle (c_ν) bins read:

$$N_{i,j,\mu} = \frac{2\pi N_T t}{V_{\text{det}}} \int_{E_i}^{E_i+\Delta_i} dE_\nu \int_{c_{\nu,j}}^{c_{\nu,j}+\Delta_j} dc_\nu V_\mu \times \left(\frac{d\phi_{\nu_\mu(\nu_e)}}{dE_\nu d\Omega} \sigma_{\nu_\mu(\nu_e)}^{\text{CC}} P_{\nu_\mu(\nu_e) \rightarrow \nu_\mu} + \frac{d\phi_{\bar{\nu}_\mu(\bar{\nu}_e)}}{dE_\nu d\Omega} \sigma_{\bar{\nu}_\mu(\bar{\nu}_e)}^{\text{CC}} P_{\bar{\nu}_\mu(\bar{\nu}_e) \rightarrow \bar{\nu}_\mu} \right), \quad (12)$$

where Δ_i and Δ_j are respectively the energy and c_ν bin widths, N_T is the number of available targets, V_{det} is the total volume of the detector, t is the exposure time, $d\phi_\nu$'s are the atmospheric (anti)neutrino differential spectra,

σ^{CC} is the CC (anti)neutrino cross section and V_μ is the effective detector volume. For a detector with cylindrical shape of radius r and height h , V_μ is given by [15]

$$V_\mu(E_\mu, \theta) = 2hr^2 \arcsin \left(\sqrt{1 - \frac{R_\mu^2(E_\mu)}{4r^2} \sin^2 \theta} \right) \left(1 - \frac{R_\mu(E_\mu)}{h} |\cos \theta| \right). \quad (13)$$

where $R_\mu(E_\mu)$ is the energy-dependent muon range in ice. For σ^{CC} we use the charged current (anti)neutrino interaction cross-sections in [25]. It is useful to note that in the relevant energy range the anti-neutrino cross-section is smaller than the neutrino cross-section by about a factor of two. This difference is what allows for the (statistical) discrimination between neutrinos and anti-neutrinos and thus between normal and inverted hierarchy in this experiment.

Equation (12) contains the atmospheric electron and muon (anti) neutrino fluxes, $\frac{d\phi_{\nu_\alpha}}{dE_\nu d\Omega}$. For the results presented in this study we use the results from Refs. [22]. The atmospheric neutrino fluxes from Refs. [23] have also been used, and, overall, we obtain a similar difference between the number of muon neutrino induced events for the normal and inverted hierarchies both in energy and c_ν . The absolute electron and muon atmospheric (anti)neutrino fluxes are found to have errors of 10% – 15% in the energy region of interest here [24]. Those errors are mostly induced by our ignorance in modeling hadron production, although the situation is expected to improve with HARP and MIPP data. The uncertainties quoted above are reduced for the neutrino-antineutrino flavor ratio case [30], i.e. for $\nu_\mu/\bar{\nu}_\mu$ and $\nu_e/\bar{\nu}_e$, where the uncertainty is $\sim 7\%$ in the energy range we explore in the current study. Even smaller uncertainties are expected when the muon-to-electron flavor ratio $(\nu_\mu + \bar{\nu}_\mu)/(\nu_e + \bar{\nu}_e)$ is considered. We will comment on

the impact of the atmospheric neutrino flux uncertainties on our results below, when including systematic uncertainties to our numerical analysis.

The energy of secondary muons from CC interaction in the 10-100 GeV neutrino energy range of interest here is $\langle E_\mu \rangle = 0.52 E_\nu$ and $0.66 E_\nu$, respectively for neutrinos and antineutrinos [25]. We illustrate in Fig. 1 the expected μ -like *contained* events in 5 GeV *muon energy* bins for a combined detector mass times exposure of 50 Mt yr. From left to right, the panels depict the contained μ -like events within the $(-1, -0.9)$, $(-0.9, -0.8)$ and $(-0.8, -0.7)$ c_ν bins. We assume $\sin^2 2\theta_{13} = 0.1$ and $\delta = 0$ along with other best-fit parameters in Eq. (8). Although we used a detector geometry of 1 km height and ~ 40 m radius, all events are contained in these c_ν bins except for the highest energy bin: (25,30) GeV. As we will shortly see, the oscillation signals solely affect the low energy events. Thus our results are valid for a variety of detector geometries, only affected by the total instrumented volume times the exposure.

For the first c_ν bin used in Fig. 1 the (anti)neutrinos are almost vertically upward going and in their way towards the detector they have crossed the high density Earth core. For the other bins (anti)neutrinos still traverse a significant amount of matter through the Earth. Note that a finer angular bin than $\Delta c_\nu \sim 0.1$ is not possible because the reconstruction of primary neutrino direction is expected to be poor in this energy range due

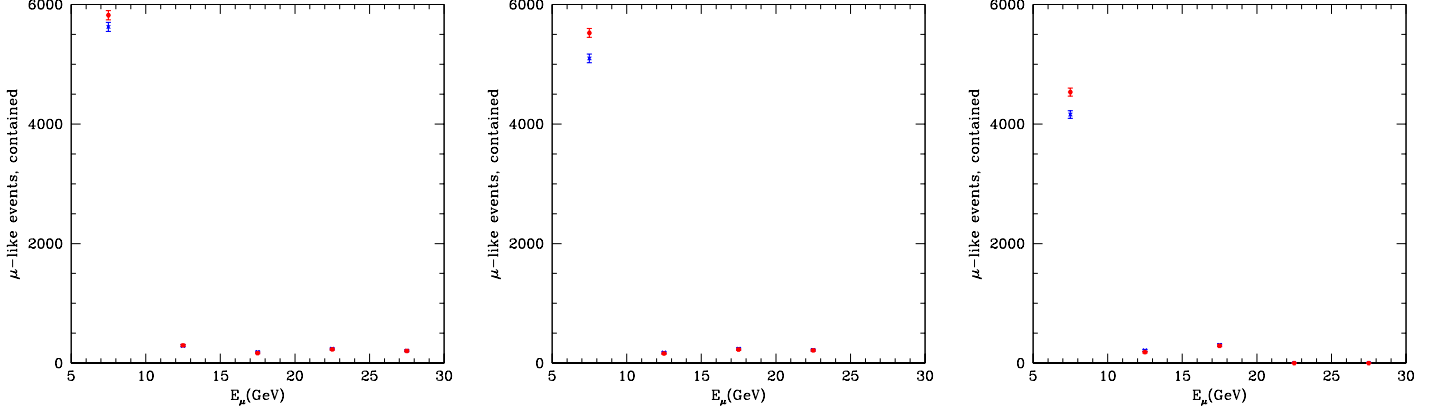


FIG. 1: From left to right, number of contained μ -like events in a 5000 kton detector after 10 years exposure, within the $(-1, -0.9)$, $(-0.9, -0.8)$ and $(-0.8, -0.7)$ c_ν bin, assuming $\sin^2 2\theta_{13} = 0.1$, $\delta = 0$ and an energy bin size of 5 GeV, with a muon energy threshold for detection of 5 GeV. We show the 1σ statistical errors. The blue crosses (red circles) denote positive (negative) hierarchy.

to the intrinsic spread in charged lepton-neutrino scattering angle. The resonance is expected to be located at low energies, see Eq. (10), and the maximum difference between normal and inverted hierarchies is observed in the (5, 10) GeV energy bin. In higher energy bins, the effect is totally negligible.

Figure 1 helps understanding the energy and angular bins that should be considered for the numerical analysis developed in the current study. We will exploit exclusively the first two muon energy bins (i.e. E_μ within the (5, 10) GeV and (10, 15) GeV energy ranges), and three angular bins, i.e., c_ν within the $(-1, -0.9)$, $(-0.9, -0.8)$ and $(-0.8, -0.7)$ ranges). It is precisely in those bins where the sensitivity to the neutrino mass ordering is significant, and all the muon events are fully contained. Since the atmospheric neutrino spectra are very steep ($\sim E_\nu^{-3}$ in the relevant energy range) and, as we will discuss next, this energy range also corresponds to a neutrino oscillation maximum, most events are concentrated in the lowest energy bin. It is thus important to keep the muon energy threshold for detection as low as possible (between 5 and 7 GeV) to collect large statistics as well as for extracting the neutrino mass ordering. We next discuss the oscillation effects in the event rates in Fig. 1. Notice that for the three angular bins illustrated here, the number of μ -like events in the first energy bin is larger for the inverted hierarchy case than for the normal hierarchy case. The reason for that is due to the presence of matter effects at these zenith angles for ν_μ 's, which are the ones dominating the statistics. This can be well seen in Fig. 2, which shows $P_{\nu_e \rightarrow \nu_\mu} (\equiv P_{e\mu})$ and $P_{\nu_\mu \rightarrow \nu_\mu} (\equiv P_{\mu\mu})$ for both normal and inverted hierarchy, for $\sin^2 2\theta_{13} = 0.1$ and $\sin^2 2\theta_{13} = 0.06$. If the hierarchy is positive (negative), the $P_{\mu\mu}$ survival probabilities, in the ~ 10 -20 GeV energy range for neutrinos (which are

responsible to produce 5-10 GeV muons), are suppressed (enhanced), due to matter effects, and therefore a smaller (larger) number of ν_μ CC interactions are expected in the detector. If the matter density is constant, and the contribution from the solar terms is negligible, the $P_{\mu\mu}$ survival probability is given by (see Refs. [13, 14])

$$\begin{aligned}
 P_{\mu\mu} = & 1 - \cos^2 \theta_{13}^m \sin^2 2\theta_{23} \\
 & \times \sin^2 \left[1.27 \left(\frac{\Delta m_{31}^2 + A + (\Delta m_{31}^2)^m}{2} \right) \frac{L}{E} \right] \\
 & - \sin^2 \theta_{13}^m \sin^2 2\theta_{23} \\
 & \times \sin^2 \left[1.27 \left(\frac{\Delta m_{31}^2 + A - (\Delta m_{31}^2)^m}{2} \right) \frac{L}{E} \right] \\
 & - \sin^4 \theta_{23} \sin^2 2\theta_{13}^m \sin^2 \left[1.27 (\Delta m_{31}^2)^m \frac{L}{E} \right],
 \end{aligned} \tag{14}$$

where $A = 2\sqrt{2}G_F N_e E$, θ_{13}^m is given by Eq. (9) and

$$(\Delta m_{31}^2)^m = \Delta m_{31}^2 \sqrt{\sin^2 2\theta_{13} + \left(\cos 2\theta_{13} \mp \frac{2\sqrt{2}G_F N_e E}{\Delta m_{31}^2} \right)^2}, \tag{15}$$

where the minus (plus) sign applies to neutrino (antineutrino) flavor transitions. Due to the presence of resonant matter effects in the first angular and energy bins, $P_{\mu\mu}$ can be very different for positive and negative hierarchies (mostly due to changes in the first term in Eq. (15)).

As seen in Fig. 2, the $\nu_e \rightarrow \nu_\mu$ probability is quite small in the relevant energy range (negligible for inverted hierarchy). Its contribution to the final muon-like event rate is made even smaller by the fact that the atmospheric ν_e flux at these energies is much smaller than the ν_μ flux. The experiment we are considering is thus mostly exploiting matter effects in the *disappearance* $\nu_\mu \rightarrow \nu_\mu$

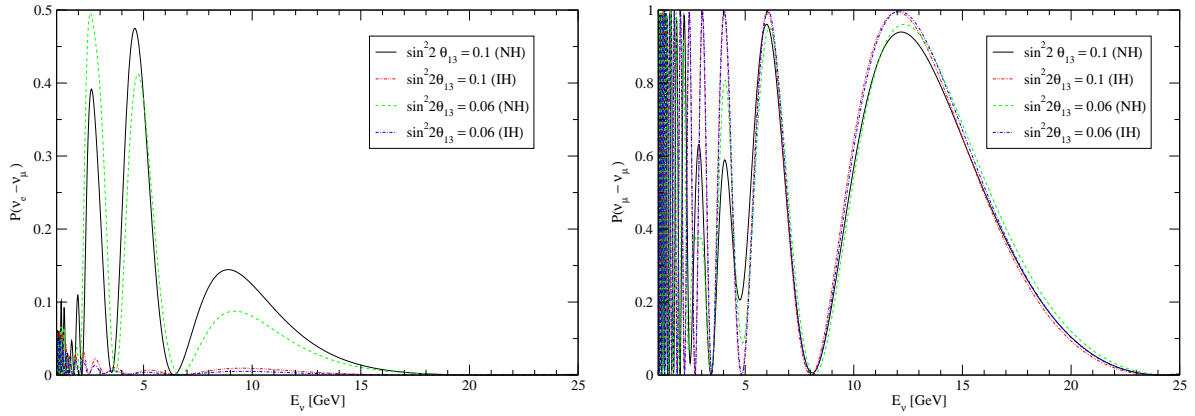


FIG. 2: left (right panel): Oscillation probabilities for $\nu_e \rightarrow \nu_\mu$, $\nu_\mu \rightarrow \nu_\mu$ transitions for $c_\nu = -1$.

channel and therefore is in many ways complementary to the appearance experiments. While the matter effects are a small correction in the ν_μ survival probability, they are sufficient to provide a difference between the different mass orderings because of the very large number of events.

Note that in Fig. 1 the difference between event rates for the two hierarchies increases (although the overall rates decreases) for c_ν bins $(-0.9, -0.8)$ and $(-0.8, -0.7)$ compared to the $(-1, -0.9)$ bin. This is because the resonant matter density for neutrino energies in the first energy bin $< E_\nu > = 15$ GeV is ~ 5 g/cm³ which is lower than the densities that the neutrino crosses if c_ν is in the $(-1, -0.9)$ region, but gets closer to the ones in the shallower c_ν region.

IV. BACKGROUNDS AND SYSTEMATIC UNCERTAINTIES

The main backgrounds to the signal we are exploiting in the current study are atmospheric downward going muons from the interactions of cosmic rays in the atmosphere and tau (anti)neutrinos from $\nu_{\mu,e}(\bar{\nu}_{\mu,e}) \rightarrow \nu_\tau(\bar{\nu}_\tau)$ transitions. The cosmic muon background can be eliminated by angular cuts and in the Ice Cube deep core is significantly reduced compared to the IceCube detector.

The tau neutrino background can be included in the analysis as an additional source of μ -like events. Tau (anti)neutrinos resulting from atmospheric neutrino flavor transitions will produce a τ lepton by CC interactions in the detector effective volume. The tau leptons produced have an $\sim 18\%$ probability of decaying through the $\tau^- \rightarrow \mu^- \bar{\nu}_\mu \nu_\tau$ channel.

The secondary muons can mimic muons from ν_μ CC interactions and must be included in the oscillated signal. The energy of a ν_τ needs to be about 2.5 times higher than a ν_μ to produce, via tau decay, a muon of the same energy. But the atmospheric neutrino flux has a steeply

falling spectrum, so one would expect this tau-induced muon background not to be very large. It is however significant ($\sim 10\%$) due to the fact that, as seen in Figure 3, the first maximum in the $\nu_\mu \rightarrow \nu_\tau$ oscillation probability (minimum in the $\nu_\mu \rightarrow \nu_\mu$ survival probability) falls exactly in the energy range of interest and for a large range the ν_τ flux can be significantly larger than the ν_μ flux. These events significantly change the energy spectrum of the measured muon-like events and contain information about the main oscillation parameters, Δ_{31} and θ_{23} .

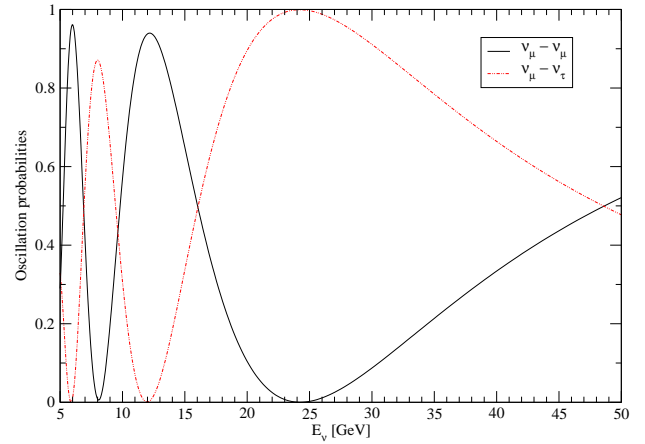


FIG. 3: ν_μ survival probability and $\nu_\mu \rightarrow \nu_\tau$ oscillation probability for $c_\nu = -1$, $\sin^2 2\theta_{13} = 0.1$

The uncertainties in the atmospheric neutrino flux have been discussed in the previous section and they affect the analysis. It is however possible to use the data itself to improve some of the errors introduced by these effects, by considering energy and angular bins where oscillation effects are not important as a reference and thus canceling out some of these uncertainties in the analysis (see also [26]).

The uncertainties in other oscillation parameters also affect the possibility of determining the neutrino mass hi-

erarchy. We employ a full three-flavour oscillation analysis. It is however easy to understand that the solar Δm^2 and mixing angle have almost no contribution. This is due to the high energy values we are considering, for which even the largest distances traveled by atmospheric neutrinos do not allow the $\Delta m_{21}^2 L/E$ term to become significant. The present uncertainties in $|\Delta m_{31}^2|$ and θ_{23} (see Eq. (8)) will be improved by present accelerator experiments. In addition, the atmospheric neutrino data in the IceCube deep core can be used to extract these parameters independently from the sub-dominant effects, by comparing different angular bins. The values of θ_{13} and δ are the most uncertain and usually hardest to disentangle from the mass hierarchy. A measurement of the θ_{13} mixing angle by the near future reactor experiments would guarantee the possibility of extracting the mass hierarchy from the atmospheric neutrino data in IceCube. We consider in our analysis a range of values for θ_{13} and δ in order to assess the parameter space for which the neutrino mass hierarchy can be determined. It is important to emphasize however that the sensitivity to the CP-violating phase δ and the value of θ_{23} in this experiment is quite small due to the fact that the signal is dominated by the ν_μ disappearance channel.

V. RESULTS

In this section we present our results in terms of a minimum χ^2 analysis in the $(\sin^2 2\theta_{13}; \delta)$ parameter space. For a particular hierarchy (h) and $(\sin^2 2\theta_{13}; \delta)$ parameters chosen by nature, we consider the number of μ -like events $N_{ij,h}^{\text{ex}}(\sin^2 2\theta_{13}; \delta)$ measured by an experiment in the i - and j -th muon energy and c_ν bins (see Eq. (12)). These events include the ν_μ and $\bar{\nu}_\mu$ signal, as well as the background secondary muons from ν_τ and $\bar{\nu}_\tau$'s.

The χ^2 statistics, for a “theoretical” model of hierarchy (h') and parameters $(\sin^2 2\theta'_{13}; \delta')$ is then defined as

$$\chi_{h'}^2(\sin^2 2\theta'_{13}; \delta') = \sum_{i=1,2} \sum_{j=1,3} \left[\frac{N_{ij,h}^{\text{ex}}(\sin^2 2\theta_{13}; \delta) - N_{ij,h'}^{\text{th}}(\sin^2 2\theta'_{13}; \delta')}{\sigma_{ij,h}^{\text{ex}}(\sin^2 2\theta_{13}; \delta)} \right]^2. \quad (16)$$

Here $N_{ij,h'}^{\text{th}}(\sin^2 2\theta'_{13}; \delta')$ is the expected event number from both signal ν_μ 's and background ν_τ 's given a “theoretical” model. The variance $\sigma_{ij,h}^{\text{ex}}(\sin^2 2\theta_{13}; \delta)$ is calculated from experimental events with or without systematic uncertainties. We minimize χ^2 in Eq. (16) for $(\sin^2 2\theta'_{13}; \delta')$ parameters (i.e. 2 d.o.f). When nature's choice or “true” hierarchy is h (normal for example), then the “wrong” theoretical model of hierarchy $h' \neq h$ (inverted in this case) is rejected if

$$\min(\chi_{h' \neq h}^2) - \min(\chi_{h'=h}^2) \geq \alpha \quad (17)$$

in the $(\sin^2 2\theta_{13}; \delta)$ parameter space. The 68%, 90%, 95% and 99% confidence levels (CL) are defined for $\alpha = 2.3$,

4.61, 5.99 and 9.21 respectively, for 2 d.o.f statistics [27]. Note that our choice of 2 d.o.f statistics is rather conservative as explained in the Appendix of Ref. [28]. Our 90% CL translate into the 97% CL for 1 d.o.f statistics.

Fig. 4, left (right) panel shows the χ^2 results in the $(\sin^2 2\theta_{13}, \delta)$ plane for a measurement of the hierarchy at the different confidence levels quoted above, exploiting the muon-like contained events in a 10000 kton detector after 10 years exposure (100 Mt yr), for positive (negative) hierarchies. The sensitivity to the mass hierarchy is better in case nature has chosen the normal hierarchy than in the case for the inverted hierarchy. The reason for that is that in the normal mass ordering scenario, matter effects decrease (increase) the muon neutrino (antineutrino) survival probability. In the inverted mass ordering scenario, matter effects decrease (increase) the muon antineutrino (neutrino) survival probability. Notice the observable we are exploiting here contains both the atmospheric neutrino and antineutrino fluxes, see Eq. (12). Since in the energy range of interest the neutrino fluxes are roughly twice the antineutrino ones, the overall effect for the normal hierarchy is larger, i.e. no significant cancellation among the effects for neutrinos and antineutrinos is present. In the inverted hierarchy case, there exists a partial cancellation and therefore the sensitivity results are not as promising as the ones for the normal hierarchy.

The dependence of the χ^2 results on the value of the CP-phase δ is extremely mild, as expected, due to the fact that the muon neutrino survival probability in matter $P_{\mu\mu}$, Eq. (15), does not depend on δ in the limit of negligible solar effects. Even when solar effects are not negligible, $P_{\mu\mu}$ in matter depends exclusively on $\cos \delta$. Consequently, one would expect the same results for δ and $-\delta$, as can be clearly noticed from Figs. 4. Also, notice how the maximum (minimum) sensitivity is reached at $\delta = 0^\circ$ ($\delta = 180^\circ$), due to the change of sign in the $\cos \delta$ function.

Figs. 5 show the equivalent to Figs. 4 but including in the χ^2 analysis performed here a 10% overall systematic error, which includes uncertainties from atmospheric neutrino fluxes and cross sections, among others. The impact of the systematic errors on the sensitivity/exclusion curves is significant, therefore, keeping systematic uncertainties below the 10% level is crucial for extracting the neutrino mass hierarchy.

We also explore the impact of the θ_{23} -octant ambiguity. Following the current 95% CL allowed limits for the mixing parameter $\sin^2 2\theta_{23}$, we illustrate here the results from our χ^2 analysis for $\theta_{23} = 40^\circ$ and $\theta_{23} = 50^\circ$. Figs. 6 show the χ^2 analysis results, including a 10% overall systematic error for $\theta_{23} = 40^\circ$. Figs. 7 show the equivalent but for $\theta_{23} = 50^\circ$.

If $\theta_{23} \neq 45^\circ$, the results for the normal hierarchy become slightly worse, since $\sin^2 2\theta_{23}$ is smaller than unity and therefore the role of matter effects in the $P_{\mu\mu}$ oscillation probability is smaller (see Eq. (15)).

For the inverted hierarchy case, the best sensitivities

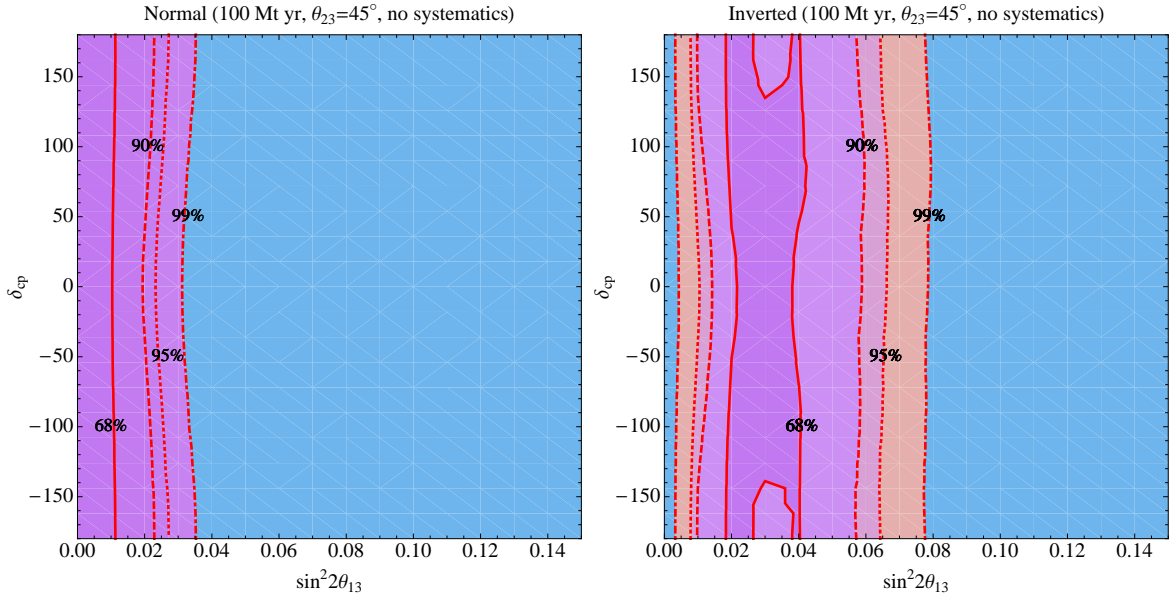


FIG. 4: Rejection regions of the “wrong” hierarchy model in the $(\sin^2 \theta_{13}, \delta_{cp})$ plane when the “true” hierarchy is normal (left panel) or inverted (right panel) as indicated in the heading of each plot. Different lines correspond to rejection regions of the “wrong” hierarchy at 68%, 90%, 95% and 99% CL (2 d.o.f.) using the muon-like contained events in a detector of mass times exposure of 100 Mt yr (e.g., 10,000 kton detector after 10 years of data taking). We used the best fit parameter values in Eqs. (1)-(4).

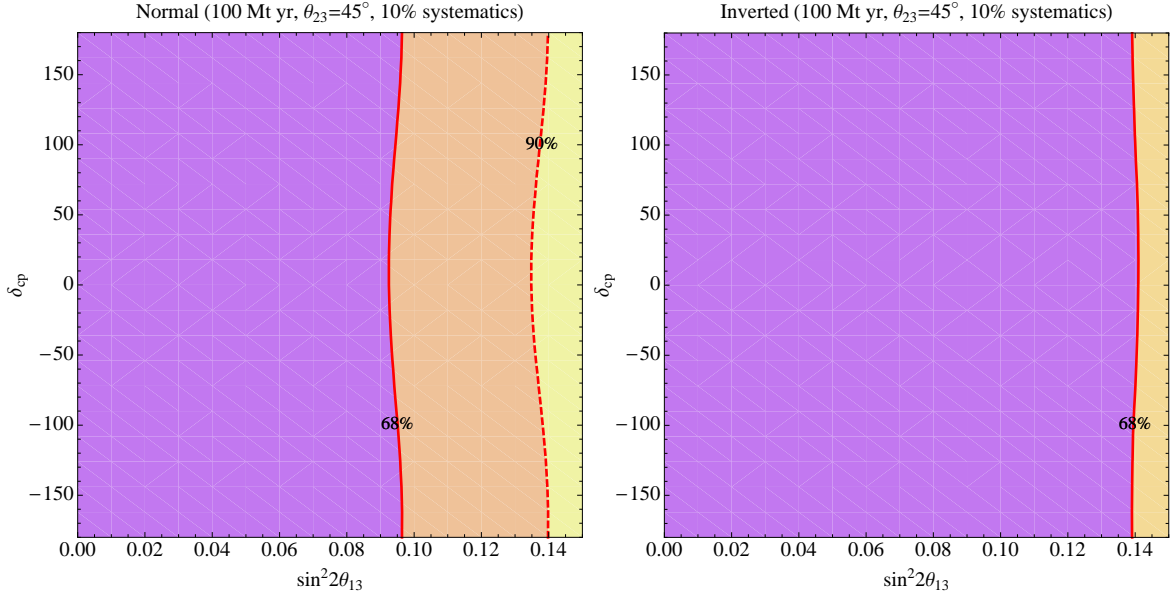


FIG. 5: Same as Fig. 4 but including a 10% systematic error in our χ^2 analysis.

are reached when $\theta_{23} = 40^\circ$. This can be understood in terms of the muon (anti) neutrino disappearance probability $P_{\mu\mu}$ in the presence of matter effects and non negligible solar effects. If one performs an expansion up to second order in the small parameters $\Delta m_{21}^2/\Delta m_{31}^2$

and $\sin \theta_{13}$, there are two terms in the muon (anti) neutrino disappearance probability equation which depend on $\cos \delta$. One term is proportional to $\sin 2\theta_{23} \cos \delta$, the other one is proportional to $\cos 2\theta_{23} \cos \delta$, and therefore it is only different from zero for $\theta_{23} \neq 45^\circ$, changing

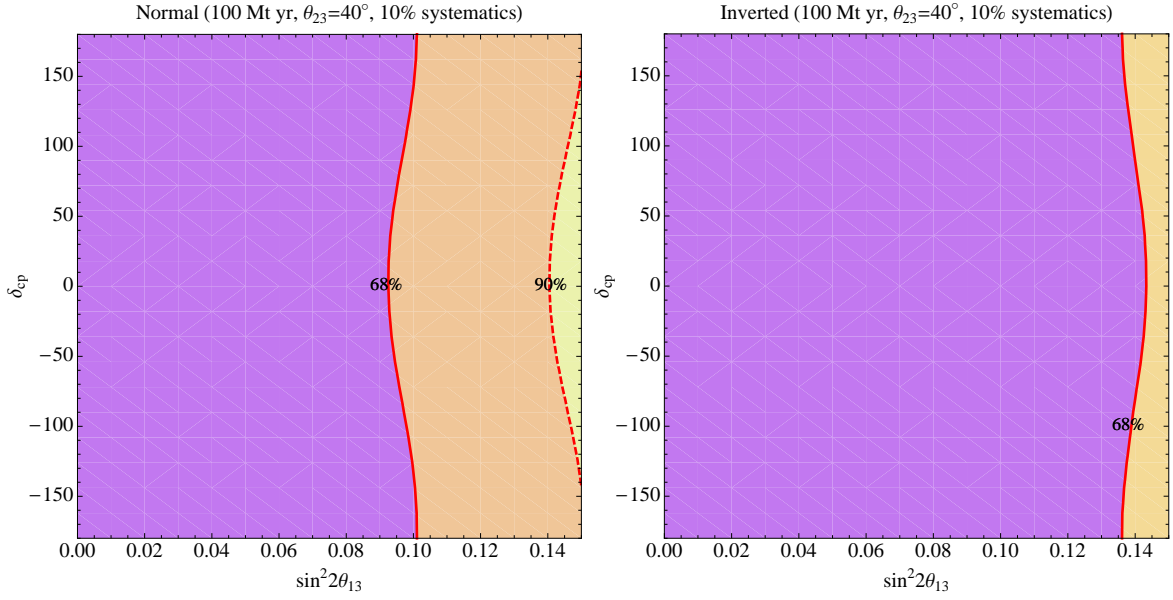


FIG. 6: Left (right) panel: the different lines depict the 68% and 90% CL (2 d.o.f.) hierarchy resolution using the muon-like contained events in a 10000 kton years detector after 10 years of data taking, for positive (negative) hierarchies, and the atmospheric mixing angle chosen to be $\theta_{23} = 40^\circ$. An overall 10% systematic error has been included in the χ^2 analysis.

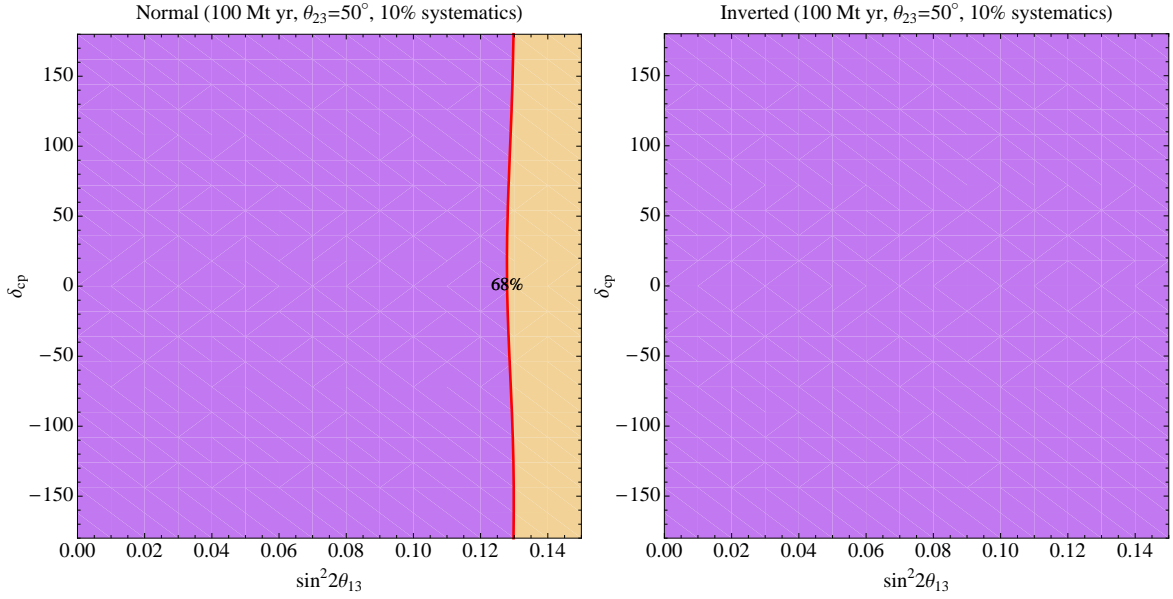


FIG. 7: Left (right) panel: the different lines depict the 68% and 90% CL (2 d.o.f.) hierarchy resolution using the muon-like contained events in a 10000 kton years detector after 10 years of data taking, for positive (negative) hierarchies, and the atmospheric mixing angle chosen to be $\theta_{23} = 50^\circ$. An overall 10% systematic error has been included in the χ^2 analysis.

its sign accordingly to the octant in which θ_{23} lies. For the muon antineutrino channel and inverted hierarchy, this term, i.e. the term proportional to $\cos 2\theta_{23} \cos \delta$ is the dominant one among the two terms proportional to $\cos \delta$ in the muon (anti) neutrino disappearance proba-

bility equation. For $\theta_{23} < 45^\circ (> 45^\circ)$, the term proportional to $\cos 2\theta_{23} \cos \delta$ maximizes (minimizes) the impact of matter effects in $P_{\mu\mu}$. The former term is also the one responsible for the change of shape in the sensitivity curves for $\theta_{23} = 40^\circ$ and for $\theta_{23} = 50^\circ$. For $\theta_{23} = 40^\circ$

the maximum is reached now at $\delta = \pm 180^\circ$ and not at $\delta = 0^\circ$. For the $\theta_{23} = 50^\circ$ case, the sensitivity curve bends in the opposite direction, due to the opposite sign of $\cos 2\theta_{23}$.

VI. DISCUSSION AND CONCLUSIONS

The IceCube detector and its proposed deep core array provide a great opportunity for studies of atmospheric neutrinos. Being the largest existing neutrino detector, it will accumulate a huge number of atmospheric neutrino events over an enormous energy range, thus allowing for detailed studies of oscillation physics, Earth density, atmospheric neutrino fluxes and new physics. In order to extract all this information it is necessary to use energy and angular distribution information, as well as flavour composition, all possible to obtain with the IceCube detector.

Qualitatively, there are three main energy intervals and three main angular regions which are sensitive to different types of physics.

At very high energies, above 10 TeV, neutrino interaction cross-sections become high enough that neutrinos going through the Earth start getting attenuated. This effect is sensitive to neutrino interaction cross-sections and to the density profile of the Earth. A measurement of the neutrino flux at these energies can provide a determination of the Earth density [29] which can be used as an experimental input to our analysis, instead of the PREM predictions.

The “intermediate” energy region, between 50 GeV and 1 TeV can provide good information about the atmospheric neutrino flux, which can be used to improve the uncertainties in the simulated atmospheric neutrino fluxes.

In our paper we concentrated on the “low” energy region, below about 40 GeV, where neutrino oscillation effects can be significant. Matter effects inside the Earth are very important in this energy range and for non-zero values of θ_{13} resonance effects can strongly enhance/reduce oscillation probabilities. Straight-up-going neutrinos ($c_\theta \leq -0.7$) pass through the core of the Earth and are most sensitive to resonant matter oscillations and thus to all sub-dominant neutrino oscillation effects (θ_{13} ,

mass hierarchy, CP violation). Up-going neutrinos at shallower angles are still sensitive to the “main” oscillation effects (Δm_{31}^2 , θ_{23}), while the other, sub-dominant contributions become smaller, due to the lower matter densities and shorter pathlengths.

In the present study we have exploited muon neutrinos and antineutrinos with energies in the 10 – 30 GeV range which have crossed the Earth (i.e. $c_\theta \leq -0.7$). Using the μ like contained events for an exposure of 100 Mton yr in the proposed Icecube deep core ice Cherenkov detector, the neutrino mass hierarchy could be extracted at the 90% CL if $\sin^2 2\theta_{13} > 0.02$ ($\sin^2 2\theta_{13} > 0.14$ when a 10% systematic error is included in the analysis) regardless of the value of the CP violating phase δ . In addition, downgoing neutrinos in the deep core will provide a measurement of the atmospheric neutrino flux, helping enormously in diminishing the systematic uncertainties [26].

The Icecube deep core array, with muon energy detection thresholds of $\sim 5 - 7$ GeV, could provide the first measurement of the neutrino mass hierarchy if $\sin^2 2\theta_{13}$ is not very small, leaving for the next generation of long baseline experiments only the extraction of the CP violating phase δ .

Acknowledgments

We would like to thank Doug Cowen, Carsten Rott and especially Ty DeYoung for useful discussions and comments. We would also like to thank Michele Maltoni for useful comments and checks of our results. OM would like to thank the precious help provided by E. Fernández Martínez for the numerical analysis. This work was supported in part by the NSF grant PHY-0555368, by the European Programme “The Quest for Unification” contract MRTN-CT-2004-503369 and by a *Ramón y Cajal* contract from MEC, Spain. SR is a National Research Council Research Associate at the Naval Research Laboratory. I.M. would like to thank the UT Austin theory group for hospitality while part of this work was being completed. This material is based upon work supported in part by the National Science Foundation under Grant No. PHY-0455649.

-
- [1] <https://www.interactions.org/cms/?pid=1009695>
 - [2] See M. C. Gonzalez-Garcia and M. Maltoni, arXiv:0704.1800 [hep-ph] for a review.
 - [3] For a recent overview, see: IceCube Collaboration, arXiv:0711.0353 [astro-ph]; and T. A. Collaboration, arXiv:0711.2683 [astro-ph].
 - [4] <http://space.newscientist.com/article/dn13190-upgraded-neutrino-detector-could-look-for-dark-matter.html>
 - [5] M. Maltoni, T. Schwetz, M. A. Tortola and J. W. F. Valle, New J. Phys. **6**, 122 (2004); G. L. Fogli, E. Lisi, A. Marrone and A. Palazzo, Prog. Part. Nucl. Phys. **57**, 742 (2006); A. Strumia and F. Vissani, arXiv:hep-ph/0606054;
 - [6] M. C. Banuls, G. Barenboim and J. Bernabeu, Phys. Lett. B **513**, 391 (2001)
 - [7] T. Tabarelli de Fatis, Eur. Phys. J. C **24**, 43 (2002)
 - [8] M. C. Banuls, G. Barenboim and J. Bernabeu, Nucl. Phys. B **669**, 255 (2003)
 - [9] S. Palomares-Ruiz and S. T. Petcov, Nucl. Phys. B **712**, 392 (2005)

- [10] A. Donini *et al.*, arXiv:hep-ph/0703209.
- [11] P. Huber, M. Maltoni and T. Schwetz, Phys. Rev. D **71**, 053006 (2005)
- [12] R. Gandhi, P. Ghoshal, S. Goswami, P. Mehta and S. Uma Sankar, arXiv:hep-ph/0506145.
- [13] R. Gandhi, P. Ghoshal, S. Goswami, P. Mehta, S. U. Sankar and S. Shalgar, Phys. Rev. D **76**, 073012 (2007).
- [14] S. Choubey and P. Roy, Phys. Rev. D **73**, 013006 (2006).
- [15] I. F. M. Albuquerque and G. F. Smoot, Phys. Rev. D **64**, 053008 (2001)
- [16] T. Tabarelli de Fatis [MONOLITH collaboration], arXiv:hep-ph/0106252.
- [17] P. Adamson *et al.* [MINOS Collaboration], Phys. Rev. D **73**, 072002 (2006);
- [18] INO Report, available at: <http://www.imsc.res.in/~ino/>.
- [19] L. Wolfenstein, Phys. Rev. D **17**, 2369 (1978); V. D. Barger, K. Whisnant, S. Pakvasa and R. J. N. Phillips, Phys. Rev. D **22**, 2718 (1980); S. P. Mikheev and A. Y. Smirnov, Sov. J. Nucl. Phys. **42**, 913 (1985); S. J. Parke, Phys. Rev. Lett. **57**, 1275 (1986); H. W. Zaglauer and K. H. Schwarzer, Z. Phys. C **40**, 273 (1988); M. C. Banuls, G. Barenboim and J. Bernabeu, Phys. Lett. B **513**, 391 (2001); M. Freund *et al.*, Nucl. Phys. B **578**, 27 (2000), I. Mocioiu and R. Shrock, Phys. Rev. D **62**, 053017 (2000).
- [20] J. Arafune, M. Koike and J. Sato, Phys. Rev. D **56**, 3093 (1997) [Erratum-ibid. D **60**, 119905 (1999)]; H. Minakata and H. Nunokawa, Phys. Lett. B **413**, 369 (1997); A. Donini *et al.*, Nucl. Phys. B **574**, 23 (2000).
- [21] A. M. Dziewonski and D. L. Anderson, Phys. Earth Planet. Interiors **25** (1981) 297.
- [22] V. Agrawal, T. K. Gaisser, P. Lipari and T. Stanev, Phys. Rev. D **53**, 1314 (1996); G. D. Barr, T. K. Gaisser, P. Lipari, S. Robbins and T. Stanev, Phys. Rev. D **70**, 023006 (2004). [arXiv:astro-ph/0403630].
- [23] M. Honda, T. Kajita, K. Kasahara and S. Midorikawa, Phys. Rev. D **70**, 043008 (2004); M. Honda, T. Kajita, K. Kasahara, S. Midorikawa and T. Sanuki, Phys. Rev. D **75**, 043006 (2007).
- [24] G. D. Barr, T. K. Gaisser, S. Robbins and T. Stanev, Phys. Rev. D **74**, 094009 (2006)
- [25] R. Gandhi, C. Quigg, M. H. Reno and I. Sarcevic, Astropart. Phys. **5**, 81 (1996); R. Gandhi, C. Quigg, M. H. Reno and I. Sarcevic, Phys. Rev. D **58**, 093009 (1998).
- [26] M. C. Gonzalez-Garcia, M. Maltoni and J. Rojo, JHEP **0610**, 075 (2006).
- [27] W. M. Yao *et al.*, Journal of Physics, G **33**, 1 (2006).
- [28] O. Mena, H. Nunokawa and S. J. Parke, Phys. Rev. D **75**, 033002 (2007).
- [29] P. Jain, J. P. Ralston and G. M. Frichter, Astropart. Phys. **12**, 193 (1999); M. C. Gonzalez-Garcia, F. Halzen, M. Maltoni and H. K. M. Tanaka, arXiv:0711.0745 [hep-ph].
- [30] In general, the different available computations of the atmospheric neutrino fluxes [22, 23] predict almost the same neutrino-antineutrino ratios.